Performance Analysis of Fuel cell Powered Electric Vehicle Using MATLAB

Rahul Prasad
Final Year,
Electrical and Electronics Departments,
Coimbatore, India

Rajendra Prasath
Final Year,
Electrical and Electronics Departments,
Coimbatore, India

Abstract- **In this research article, a proton exchange membrane fuel cell (PEMFC) is instrumented as an electrical generator that utilizes hydrogen gas as fuel and air as an oxidizing agent to perform photoelectricity through electrochemical reactions simulated in MATLAB-Simulink environment. Most of the model is based on specifications with direct real-world significance, with a focus of going beyond empirically reporting the features of the fuel cell. Further exploration manifested that the execution of the PEMFC depends on the air supply pressure and rate of fuel supply. The output voltage and current waveforms from the fuel cell stack and the lithium-ion battery's efficiency and voltage waveforms are plotted as well. We also designed the powertrain systems required for a Fuel cell powered electric vehicle. The Fuel cell vehicle presented draws its power from the hydrogen powered fuel cell instead of relying on a separate battery. Electric Vehicle parameters such as speed and distance have also been plotted showing the efficiency and performance of the system. Obtained results under MATLAB/Simulink and some experimental ones are presented and discussed.**

Index Terms- Electric Vehicle, Fuel Cell, MATLAB-Simulink, Simulation

I. INTRODUCTION

Development of substitute green power sources is essential to replace the existing need for fossil fuels in order to minimize its harmful effects on the environment and health. Among the substitutes, the fuel cell technology is an encouraging replacement source of energy for sustainable development. Conventional fuel sources are responsible for the rapid climate change as well as global warming. On the contrary, fuel cell does not emit any harmful gases or substances such carbon monoxide, carbon dioxide etc. Fuel cell converts chemical energy to electrical engine unlike the conventional engines which convert fossil fuels in to heat and light energy. Among the several kinds of fuel cells available, proton exchange membrane fuel cell (PEMFC) is used widely because of its characteristics such as high efficiency, fast startup and ability to perform at low temperatures. Having a lifespan of 5000 h and a high-power density (0.3–0.8W/cm2), PEMFC is perfectly suited for electric vehicles. However, the PEMFC has the limitations of having sensitivity to carbon monoxide (CO) and the use of costly platinum catalyst [1].

Some the primary uses of fuel cells are in commercial, industrial, and residential structures, as well as remote or inaccessible places, require primary and backup electricity. They can also be used to power fuel cell vehicles such as fort lifts, automobiles, buses, boats etc.

A typical PEM fuel cell has the following reactions:

At the Anode: H2(gas)→2H++2e−H2gas→2H++2e−

At the Cathode: ½O2(gas)+2H++2e−→H2O (liter)

Overall Reaction:

H2(gas)+½O2(gas)→H2O
(liter)H2gas+½O2gas→H2Olitre

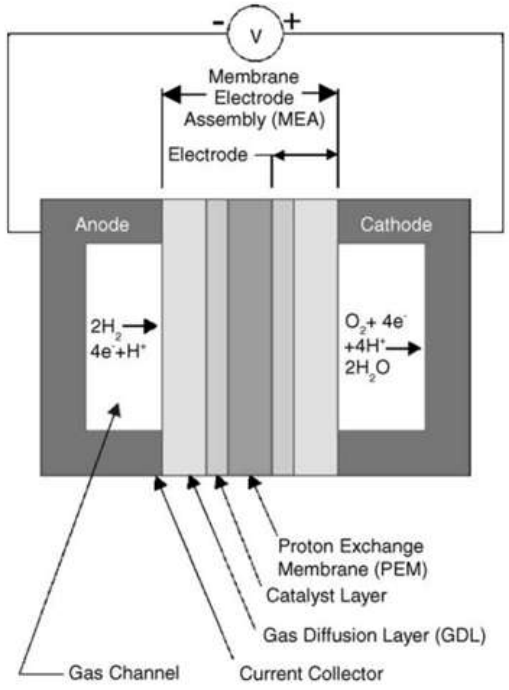

Fig. 1. Typical PEM Fuel cell

FCEVs are not currently available for purchase. The absence of sufficient hydrogen infrastructure and the high prices of the FC motor train are the key issues. FCEVs compete with both ICE-powered vehicles and other electrical cars[10]. FCEVs have been successfully driven for millions of miles. The vehicles' performance and reliability are both sufficient for production. However, other technological breakthroughs are still required, such as an increase in the FC system's lifetime. The cost of the FC drive train is a much more difficult problem to solve. FCEVs driven by hydrogen, as well as the architecture to power them, are still in the early stages of implementation and marketing for civilian use, with limited

numbers of test cars available for select enterprises with access to hydrogen fueling stations.

II. LITERATURE REVIEW

Sir William Grove created the first fuel cell in 1839. He utilized copper, sheet iron, and porcelain plates, as well as a copper sulphate and weak acid solution. [3]. In 1950, Francis Bacon of Cambridge University created the first alkaline-based workable fuel cell. The fuel cells in Windsor devised a fuel cell power plan for the Apollo Spacecraft in the 1960s, which would supply both water and energy on their voyage to the moon. [4]. Pratt & Whitney obtained US patents for use in the US space program to provide power and water in the 1960s. Roger Billings created the first hydrogen fuel cell vehicle in 1991. [5]. UTC Power was the pioneer firm to develop and sell a large utility - scale fuel cell system to be used in healthcare, colleges, and major commercial buildings as a power generation station.

Around 1959, The very first modern fuel cell automobile was a customized Allis-Chalmers agricultural tractor with a 15-kilowatt fuel cell. [11]. The Electro van, built by General Motors in 1966, was the first fuel cell road vehicle which ran on a PEM fuel cell. As of December 2020, there were 31,225 hydrogen-powered passenger FCEVs on the road across the world. The country having the most passenger FCEVs is South Korea followed by the United States, China, and Japan. There was minimal hydrogen infrastructure in the United States as of 2020, with less than fifty hydrogen refueling stations for vehicles accessible to the public.[12]

The fundamental distinction between FCEVs and BEVs is the main energy source. While FBEVs operate on battery, Fuel cell Electric vehicles rely on fuel cells, which have several advantages over batteries. Fuel cells have the advantages of being lighter and smaller, as well as the ability to generate energy as long as the fuel is available.

For automobile use case, PEMFC is the best choice available. Because fuel cells create energy through chemical processes rather than combustion, they do not emit pollutants and create less heat [10]. A hydrogen fuel cell produces water as a byproduct. Because there are no moving components or unusual forms in fuel cells, they offer the potential for excellent dependability and cheap production cost.

III. PROPOSED DESIGN AND METHODOLOGY

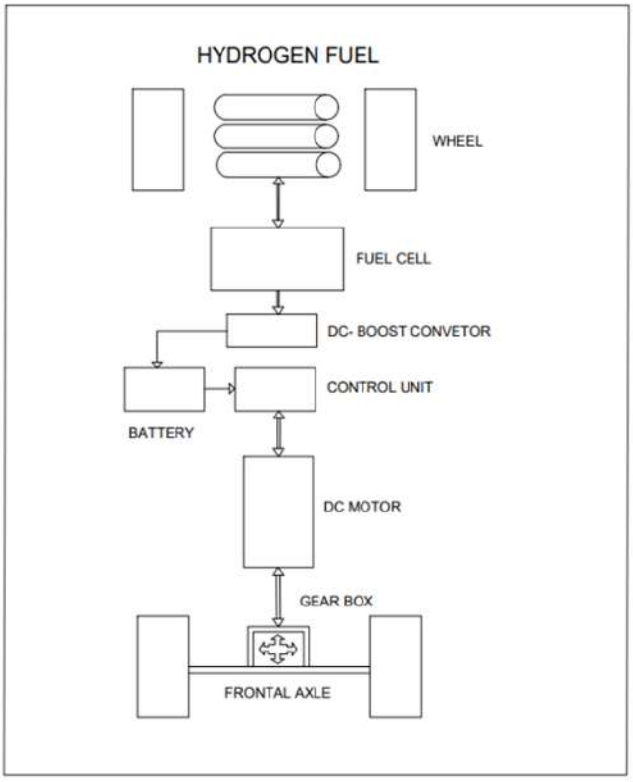

Fig. 2. Model diagram for FCEV

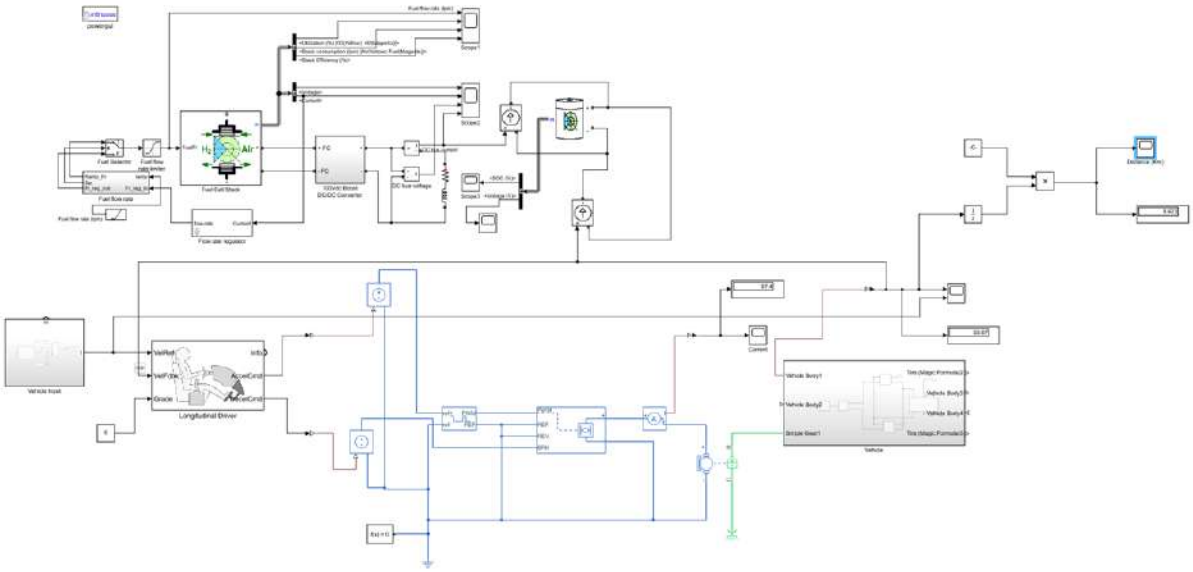

Fig. 3. Simulation Model

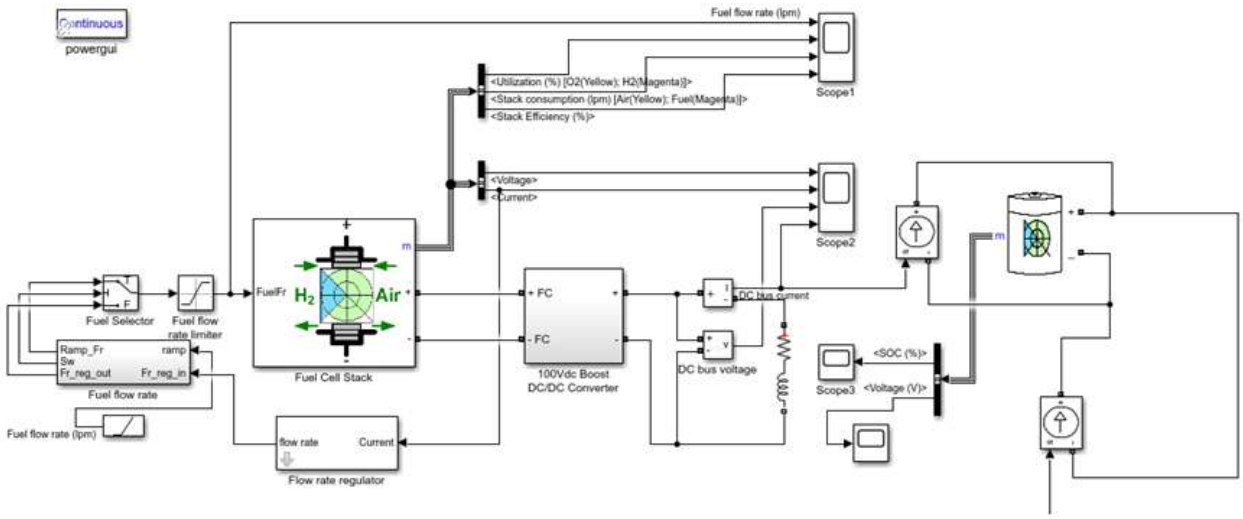

Fig. 4. Fuel cell model

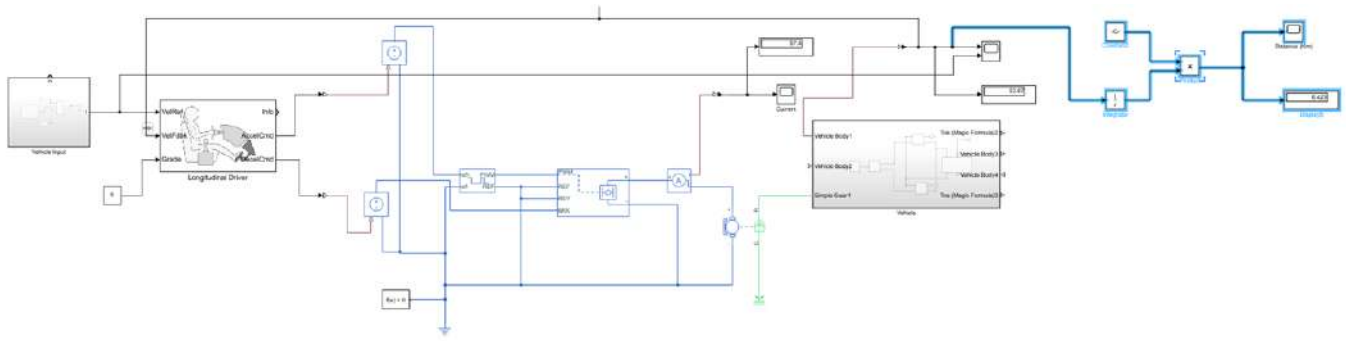

Fig. 5. Car Model

A.

B. System Components

Cell system design is complicated, and it varies greatly depending on the application and fuel cell type. 65 PEMFCs (65 FCs connected in series), a DC-DC converter, a flow regulator, a flow selector, a battery, and other components are included in the proposed system. PID controllers govern the system output voltage at 48Vdc by controlling the hydrogen and air flow rates. The battery is then linked to the vehicle. A driver input, controlled PWM voltage, H-bridge, DC motor, and the vehicle (body) are all part of this planned car system.

- Fuel cell

The Fuel Cell block incorporates a comprehensive model to constitute the most common models of hydrogen and air-fueled fuel stacks. The block shows 2 types of stack models:

A simple model - Which is not going to be utilized to depict a specific fuel cell working at hypothetical temperature and pressure conditions.

A detailed model - Which will be used to act for a specific fuel cell stack operating at theoretical temperatures and pressures. A detailed model is added simulate a precise fuel stack when conditions such as temperature, pressure, fuel flow rates, composition, and air change. The PEMFC-6KW-45Vdc type Stack model is used in this model.

- Flow Rate Regulator

This block is made up of two parts: saturation and function. This block is also known as a flow rate regulator, and it serves as a feedback element in this model, taking input from the output current and feeds it to the controller. There is a math equation block in this collective block that establishes the relationship between output and input flow rate.

$$\frac{60000 * 83145 * (273 + T) * Nc * \mu(1)}{2 * 96485 * (Pf * 101325) * U \frac{fH\text{^}2}{100} * \frac{x}{100}}$$

- Fuel Flow Rate

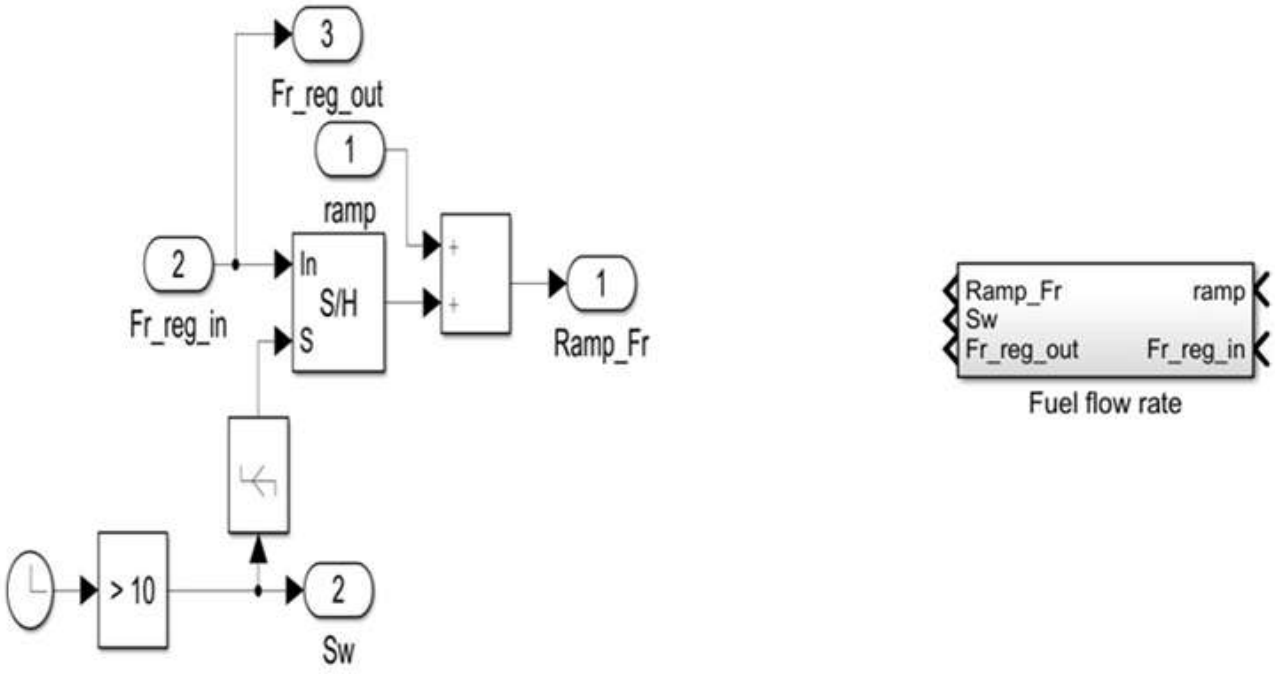

Fig. 6. Fuel Flow Model

A clock is included in the circuit, which displays the current simulation time. A compare to constant block is built up, allowing the signal to start after 10 seconds because the > 10 operator is used, and passing it to the Edge Detector, which detects a change of 10. The signal is now passed to the Sample and Hold block, where it is held and passed to the values. In this circuit, the input is 2(Fr_reg_in), and if it does not satisfy, it will go to 3(Fr_reg_out).

- Fuel Selector

When input 2 meets the set requirement, the output from Fuel flow rate passes via input 1; otherwise, it passes via input 3. From top to bottom, the inputs are numbered. The data port is the first input port, and the control port is the second input port. Control port 2 has the following criteria: u2 >= Threshold, u2 > Threshold, or u2 = 0.

The output from the Fuel flow rate system flows through input 1 of the Fuel selector since the Threshold voltage is set to 0.

- Fuel Flow Rate Limiter

The input signal is then limited to the upper and lower saturation values. The higher saturation value is set to 85, whereas the lower saturation value is retained at 0 in this case.

- 100 Vdc Boost Converter

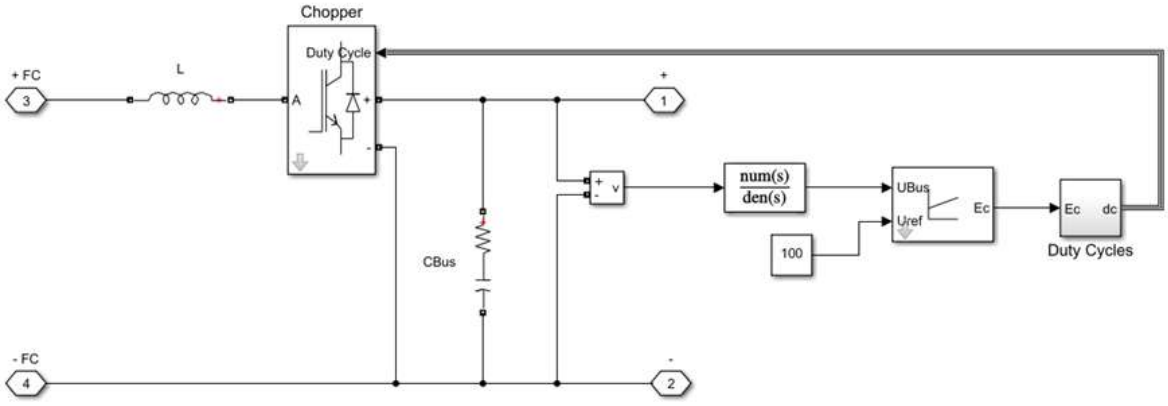

Fig. 7. 100 Vdc Boost Converter

While its input could be a very low voltage, a DC DC boost converter is used to regulate the output voltage at a high constant DC voltage to fulfil the requirement. A single chopper circuit is used in this block to maintain a consistent output

voltage of 100V. It is accomplished by fine-tuning the duty cycle.

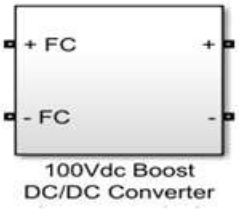

- Battery

A battery is a power source consisting of one or more electrochemical cells. We have used Lithium-Ion type battery, since it is more efficient than other type of batteries. This battery implements a generic battery model for most popular battery types. Temperature and aging (due to cycling) effects can be specified for Lithium-Ion battery type. The nominal voltage of the battery is 48Vdc, with rated capacity with 2083 Ah keeping its initial state of charge at 60%.

- Driver Input

The automobile receives information from this block. A drive cycle source, signal builder, multiport switch, and longitudinal driver are all included in this block. Multiple input sources are used so that we may test the car's performance with different input. The vehicle's longitudinal speed is the block's output. The input signals corresponding to the shortened value of the first input are passed through a multiport switch. From top to bottom, the entries are numbered. Control is the first input port. Data ports make up the rest of the inputs. The longitudinal driver is a longitudinal controller which tracks speed that uses reference and feedback velocities to generate normalized accelerating and braking commands. External actions are used to send signals to the block, which can be used to disable, hold, or override the closed-loop orders.

- Controller PWM Voltage

The PWM and REF ports are used to generate a Pulse-Width Modulated (PWM) voltage. When the pulse is small, the output voltage is zero, and when the pulse is large, it is sufficient to the Output voltage intensity factor. Input value is determined by the duty cycle. Only if the duty cycle is reduced to 0 or the pulse latency duration is larger than zero, the pulse is fired as high at zero time. This model's simulation method is configured to PWM.

- H-Bridge

An H-bridge motor drive is represented by this block. The block can be driven in PWM by the Controlled Voltage block. If the PWM terminal voltage is greater than the Enabled applied voltage, the motor is operated in PWM mode. Regulated Voltage and H-Bridge components should have the same Modeling type attribute values. The output polarity is reversed if the REV port voltage is higher than the Reverse threshold value. If the terminal voltage surpasses the Stopping voltage level, one bridge arm in series with a parallel connection of a second bridge arm and a freewheeling device short-circuits the output ports.

- DC Motor

A DC motor's The Counter-electromotive force and torque parameters have similar quantitative score in SI system since no electromagnetic energy is lost in the block. No-load speed and stall torque can be used to calculate motor parameters. This option can be set to a tiny non-zero value if there is no data on armature inductance is accessible. When a current is provided from the electrical positive to the negative terminals, the mechanical C to R ports experience a positive torque.

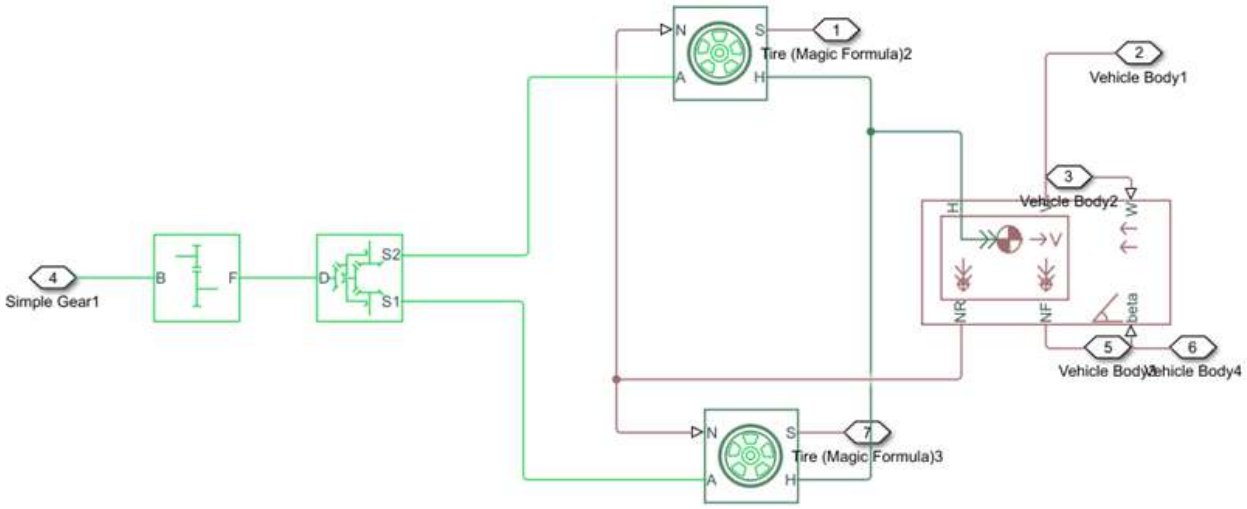

- Vehicle Model

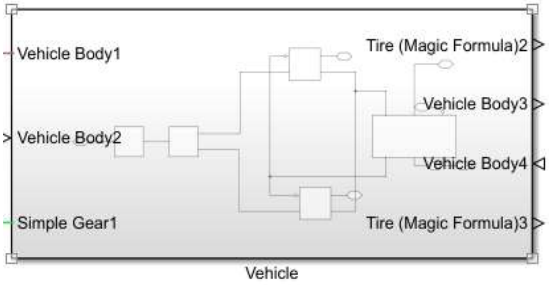

Fig. 8. Vehicle Model

Simple gear, differential, tire and vehicle body make up this block. There is no inertia or compliance modeled in this block for a Simple gear box. You can incorporate gear meshing and viscous bearing losses as options. Mechanical rotational ports are connections B (base) and F (follower). With the output shaft rotates parameter, you can specify the relationship between base and follower rotation directions. Set Friction model to a temperature-dependent option to include thermal effects and expose thermal preserving port H. A differential is a planetary bevel gear train with an additional bevel gear transmission between the driveshaft and the carrier. The transmission's pinion gear is coupled to the driveshaft, while the carrier's massive bevel crown gear is coupled to the carrier. This block does not include a compliance model. Include inertia as well as losses from gear meshing and viscous bearing friction if desired. Mechanical rotational conserving ports D, S1, and S2 are connected to the driveshaft and the two output shafts, correspondingly. The shafts of the two solar gears are S1 and S2. If the crown gear is placed to the right of centerline and there is no relative slippage across the differential, ports S1 and S2 both rotate in the positive direction while port D rotates in the positive direction. Set Friction model to a temperature-dependent option to include thermal effects and expose thermal preserving port H.

The Tire Magic Formula is used to describe the longitudinal behavior of a highway tire. The mechanical port that conserves rotation on the wheel axle is Connection A. H is the wheel hub's preserving port through machine translation via which tire's push is transferred to the vehicle. The normal force acting on the tire is applied by Connection N, a physical signal input port. If a force acts downwards, it is termed positive. The tire slip is reported by connection S. Set Parameterize based on the coefficients of the Equation for Physical Signals to reveal physical terminal M.

Due to acceleration and road profile Bodyweight, drag coefficient, surface slope, and axle center of gravity are all taken into account by the block. Each axle might have the same number of wheels or a different number of wheels. In relation to the ground, the vehicle does not move vertically. Connection H is the horizontal motion of the vehicle's body's mechanical translational conserving port. This port should be connected to the traction motion created by the tires. The CG and M physical signal input ports are open when variable mass is modelled. The extra mass is denoted by the letter M. Physical signal port J accepts the extra mass's inertia around its own CG when both variable mass and pitch dynamics are present.

IV. RESULTS AND DISCUSSION

Simulation 1

Simulation time: 20 seconds

The DC-DC boost converter applies 100Vdc to the RL load at t = 0 next 3.5 seconds. As a result of the increased DC bus voltage, the fuel cell current decreases automatically. As a result, efficiency will improve and stack consumption will reduce (Scope1).

The generated voltage is used to charge the battery linked to the boost converter throughout this simulation. Scope3 thus has the state-of-charge and consequently the voltage of the battery values seconds; the load is originally declared to be at 0A. The fuel (Hydrogen) usage is around 99.56 percent, which causes the current to rapidly climb and reach a peak current value 133A. The flow is then automatically adjusted to maintain the nominal fuel usage. Boost converter-regulated bus voltage reaches a peak value of almost 122Vdc at the voltage regulator's transient state causes this at the start of the simulation. The rate of fuel flow has been raised from 50 liters per minute (lpm) to 85 liters per minute (lpm) at t = 10 seconds, while the hydrogen usage is lowered for the next 3.5 seconds. As a result of the increased DC bus voltage, the fuel cell current decreases automatically. In turn, efficiency will improve and stack consumption will reduce (Scope1).

The generated voltage is used to charge the battery linked to the boost converter throughout this simulation. Scope3 thus has the state-of-charge and consequently the voltage of the battery values.

SCOPE 1:

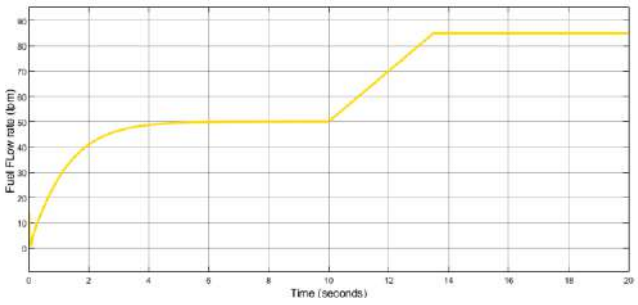

Fig. 9. Fuel Flow Rate (lpm) vs Time (sec)

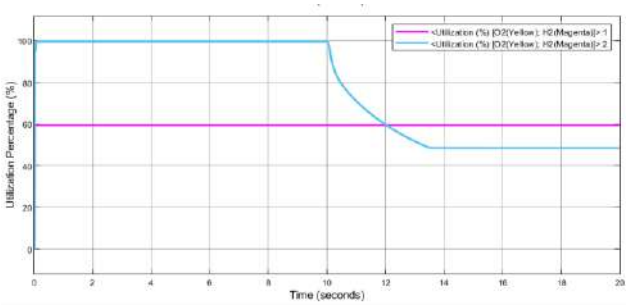

Fig. 10. Utilization of O2 with respect to H2 and (%) Time(sec)

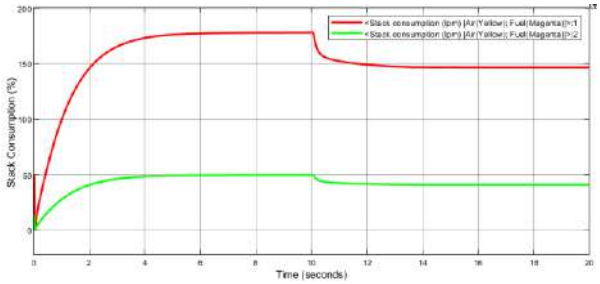

Fig. 11. Stack Consumption (%) vs Time (sec)

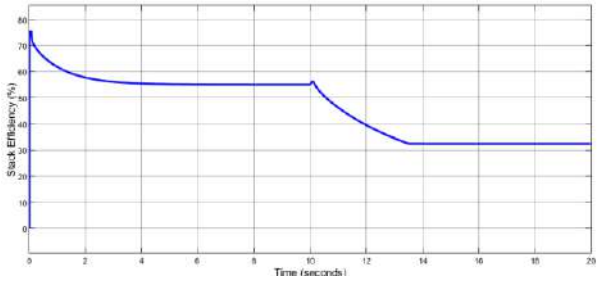

Fig. 12. Stack Efficiency (%) vs Time (sec)

SCOPE 2:

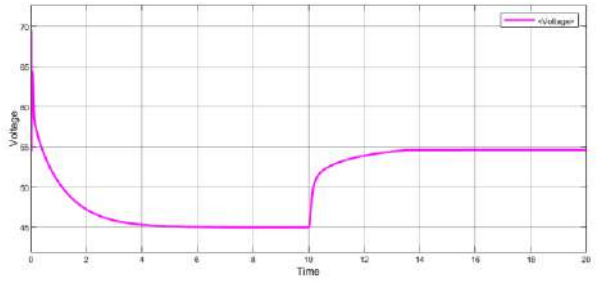

Fig. 13. Fuel Cell Voltage vs Time

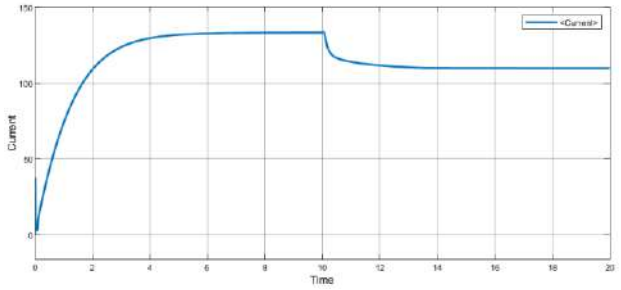

Fig. 14. Fuel cell Current vs Time

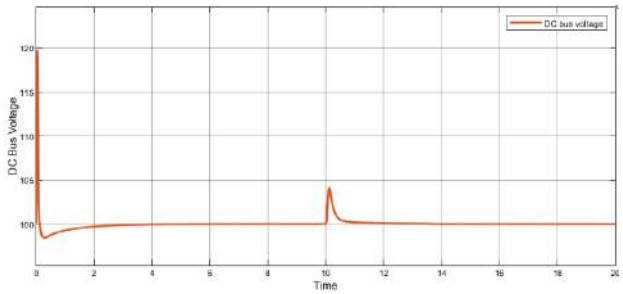

Fig. 15. DC Bus Voltage vs Time

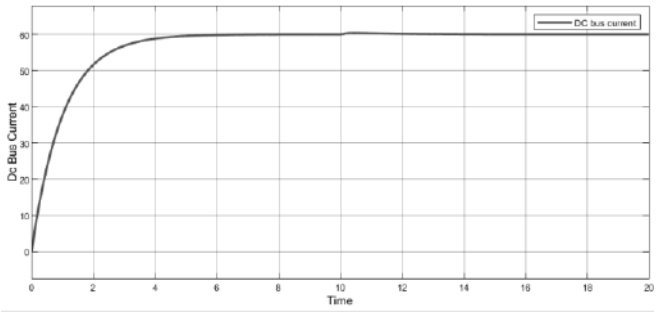

Fig. 16. DC Bus Current Vs Time

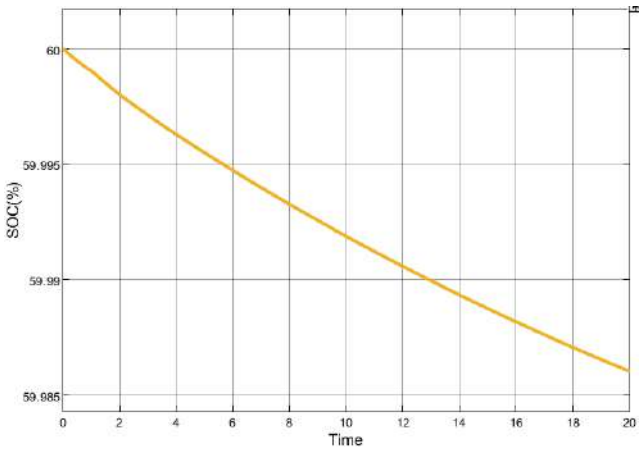

Fig. 17. State of charge vs Time

The flow is increased in the first 10 seconds and remains constant until it reaches 50 lpm, as shown in **Figure 9.** Within 3.5 seconds after 10 second mark, the flow is increased to 85 lpm. **Figure 9** shows that as the fuel flow rate is increased to 85 lpm, the utilization of hydrogen decreases from 99.56 percent to 48.315 percent.

Oxygen, on the other hand, remains constant at 59.3 percent. **Figure 10** shows that the hydrogen and oxygen consumption steadily increase and remains constant up to 10 seconds. The consumption of oxygen and hydrogen reduces after 10 seconds and remains steady. As seen in **Figure 11**, the efficiency increases at time t=0, then drops, and finally remains constant due to the transitory condition. Efficiency drops with steady stack consumption and remains constant after 10 seconds.

Figures 12, 13, 14 and **15** show that the voltage value decreases for the first 10 seconds, but increases after that when the fuel flow rate is raised. The current value of the fuel cell has been reduced to compensate for this. The battery's state of charge is increasing from its original state, as seen in **Figures 16** and **17**. (initial state of charge of battery is 60 percent). In addition, the voltage is steadily increased.

Simulation 2:

Simulation time: **600** seconds

Scope 4:

:

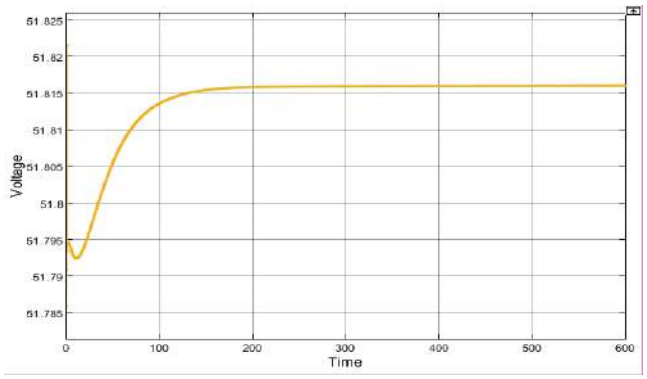

Fig. 18. Voltage(V) Vs Time

F

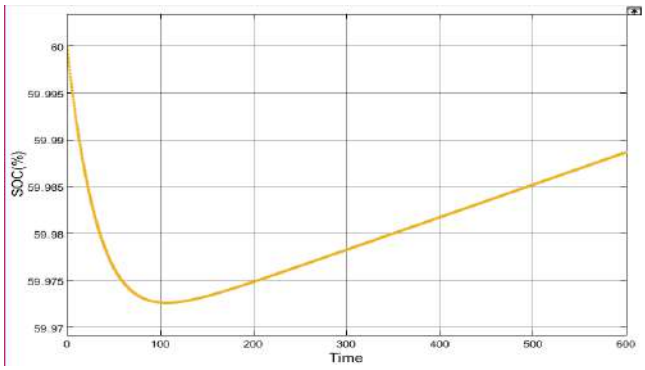

Fig. 19. State of Charge (%) Vs Time

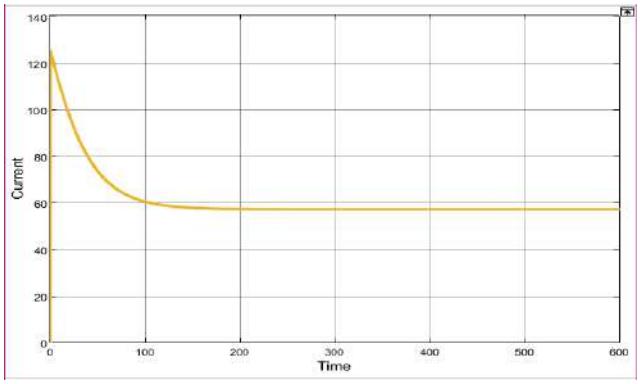

Fig. 20. Current(A) Vs Time

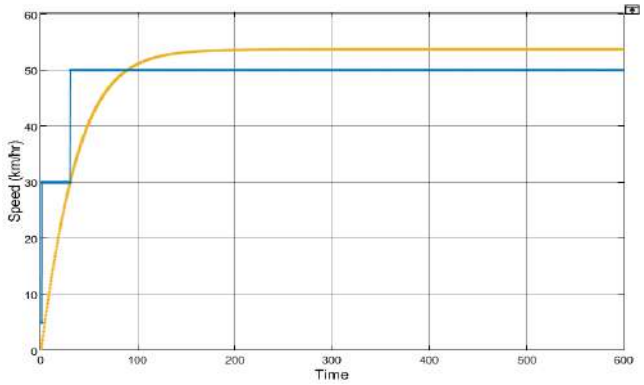

Fig. 21. Speed (km/hr) Vs Time

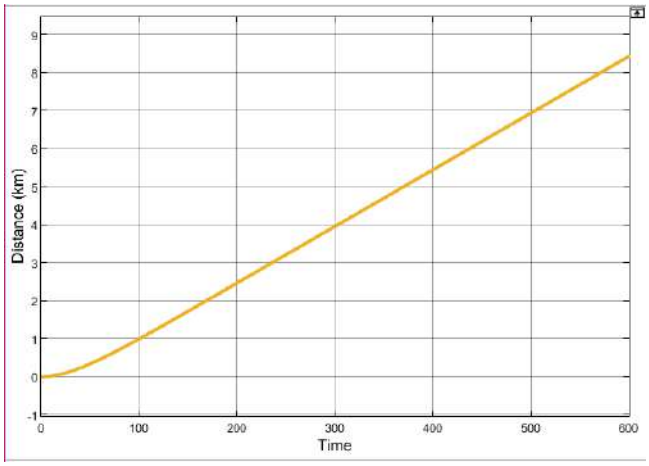

Fig. 22. Distance(km) vs Time

Figures 18 and **19** depict the battery's voltage and state of charge, respectively. As previously stated, the initial state of charge was retained at 60%. The battery percentage decreases somewhat for the first 100 seconds, but it gradually increases after that as the fuel cell continues to charge it. Figure 13 shows that current initially reaches a peak of 124A, but then steadily falls and remains constant after 100 seconds. Figure 14 depicts the speed differential between the input (drive cycle source) and output (motor speed).

Figure 20 shows the distance travelled during the simulation. We can see that the motor output speed progressively reaches its peak value and even exceeds it because we set the maximum speed (50km/hr) at 30 seconds in the drive cycle source. After 600 seconds (10 minutes) of simulation, the car has travelled 8.4 kilometers at an average speed of 48 kilometers per hour, which is rather impressive.

V. CONCLUSION

The FC system was studied in this work by modelling its dynamic behavior to obtain voltage using a boost converter. Its ability to create the desired volume has been confirmed. The simulation findings suggest that FC systems can generate voltage without incurring additional costs. We've also been able to power an automobile off the battery linked to the converter. The car model has also showed promising results, indicating that this could be the vehicle of the future. Based on these findings, we may upgrade this system in the coming years by connecting an inverter instead of a battery and a car model to convert DC to AC and connecting it with a step-up transformer to increase the generated voltage, which can then be used to supply the grid as a continuous power supply. In MATLAB/SIMULINK, dynamic simulation and modelling were performed, and the results were good.

These prospects are largely dependent on reliable and pricey high-purity hydrogen resources, the availability of more efficient competitive energy sources, and social considerations such as health and environmental benefits, as well as infrastructure development aspects associated with traditional power source and requirement and implementation scale. PEMFC has the most potential applications in buses, recreational vehicles, and lightweight vehicles, according to the

assessment. Without a question, the technologies for a consistent supply of high-purity hydrogen, as well as the infrastructure that supports it is critical to the success of PEMFC in a variety of applications.[6]

REFERENCES

[1] Kousik Ahmed , Omar Farrok , MD Mominur Rahman, Md Sawkat Ali, Md Mejbaul Haque,Abil Kalam Azad Proton Exchange Membrane Hydrogen Fuel Cell as the Grid Connected Power Generator

[2] Hydrogen and Fuel Cell Benefits http://chfcc.org/resources/hydrogen-fuelcell-benefits/Fiano C Taylor, Suresh Kumar, 2012. Stroke in India Fact Sheet. IIPH Hyderabad.

[3] Mr. W. R. Grove on a new Voltaic Combination". The London and Edinburgh Philosophical Magazine and Journal of Science. 1838. doi:10.1080/14786443808649618. Retrieved 2 October 2013.Li Zheng. 2003 Using Robotic Hand Technology for the rehabilitation of Recovering Stroke Patients with Loss of Hand Power.

[4] D.Morsi Ali,S.K. Salman A COMPREHENSIVE REVIEW OF THE FUEL CELLS TECHNOLOGY AND HYDROGEN ECONOMY Robert Gordon University, UK.

[5] "Roger Billings Biography". International Association for Hydrogen Energy. Retrieved 8 March 2011. [

[6] Jung Ho Wee. Applications of proton exchange membrane fuel cell Department of Chemical and Biological Engineering, Korea University, 1, 5-Ga, Anam-Dong, Seongbuk-Gu, Seoul,136-701, Republic of Korea

[7] Wang, C.; Nehrir, M.H.; Gao, H. Control of PEM fuel cell distributed generation systems. IEEE Trans.Energy Convers. 2006, 21

[8] El-Sharkh, M.Y.; Rahman, A.; Alam, M.S.; Byrne, P.C.; Sakla, A.A.; Thomas, T. A dynamic model for a stand-alone PEM fuel cell power plant for residential applications. J. Power Sources 2004, 138

[9] Zhang, Y.Y.; Zhang, Y.; Li, X.; Cao, G.Y. Control design of 60 kW PEMFC generation system for Residential applications. J. Zhejiang Univ.- Sci. A 2013

[10] B.G. Pollet, ... V. Molkov, in Alternative Fuels and Advanced Vehicle Technologies for Improved Environmental Performance, 2014

[11] Wand, George. "Fuel Cell History, Part 2" Archived 2015-04-02 at the Wayback Machine. "Fuel Cell Today", April 2006

[12] International Energy Agency (IEA), Clean Energy Ministerial, and Electric Vehicles Initiative (EVI)(2021-04-29). "Global EV Outlook 2021: Accelerating ambitions despite the pandemic". International Energy Agency. Retrieved 2021-05-17. Go to the Global EV Data Explorer tool and choose "EV Stock", "Cars" and "World" for global stock, and "Country" for the country stock.